Nonvascular Proton MRI of the Thorax: Pulmonary Utility and Beyond

Jonathan H. Chung, M.D.[1]; Jürgen Biederer, M.D.[2]; Michael Puderbach, M.D.[3]; Bradley D. Bolster, Jr., Ph.D.[4]; David A. Lynch, M.D.[1]

[1] Department of Radiology, National Jewish Health, Denver, CO, USA
[2] Radiologie Darmstadt, Gross-Gerau County Hospital, Gross-Gerau, Germany
[3] Department of Diagnostic and Interventional Radiology, Hufeland Klinikum GmbH, Bad Langensalza, Germany
[4] Siemens Medical Solutions, Malvern, PA, USA

Introduction

Many still perceive thoracic MRI as an exotic tool. Radiography and CT are the accepted modalities to image lung disease. However, regular use of ionizing radiation must be minimized given the risk of radiation-induced malignancy. Patients with chronic pulmonary disease can be exposed to radiation doses exceeding 100 mSv if regularly imaged with chest CT. Though the risk of most radiation-induced malignancies is substantially decreased in older individuals, this decrease does not occur in the setting of lung cancer, as the risk of lung cancer induction from radiation exposure appears to increase with age up to at least middle age [1].

The potential of MRI for scientific and clinical applications within the thorax, even beyond being a radiation-free alternative to radiography and CT, is widely underestimated. Thoracic MRI has much untapped promise in the detection and diagnosis of both focal and diffuse thoracic conditions. In the recent past, pulmonary conditions were difficult to assess using proton MRI due to low pulmonary proton density and a large degree of susceptibility artifact. Improvements in MRI technology have obviated many of these obstacles; liberal use of parallel imaging, increased gradient strength, 3D imaging, and volume interpolation now allow for reliable and high-quality imaging of the lung parenchyma using proton MRI. Chest MRI is readily available for the initial evaluation of those most at risk for the stochastic effects of radiation (children, young adults, and pregnant women) and those in whom frequent follow-up examinations are anticipated (chronic lung diseases and infections).

MRI approach

The keys to wide-spread clinical use of any tool are practicality, speed, and robustness. Our general chest MRI protocol is listed in Table 1 and shown in Figure 1. Given the inherent high soft tissue contrast of MRI, intravenous Gadolinium contrast is only optional, though administration of contrast does aid assessment of pulmonary perfusion and focal lesion enhancement while improving the overall contrast in the chest. Available MRI sequence techniques include multiple MRI weightings (T1, T2, T2/T1 ratio) in the axial and coronal planes. Though most MRI acquisitions for thoracic assessment are of good quality, some series may not be of diagnostic quality in highly dyspneic or claustrophobic patients. Our protocol ensures that adequate imaging of the thorax will occur in at least one series, even in these challenging patients. Total scan time in most cases is less than 20 minutes; a focused examination may take as little as 5 minutes once the patient has been positioned in the MRI scanner.

The VIBE sequence is a rapid T1-weighted sequence which can be acquired in one breathhold. In the setting of lung pathology, VIBE is most useful for identification of conditions which increase proton density: Pulmonary nodules, masses, and consolidation. After contrast administration, this sequence also has excellent angiographic capacities. Well in line with the concept of a simple, fast, and robust protocol design, two fast breathhold-acquisitions in coronal and transverse orientation within the first 5 minutes after administration of the contrast material produce a high quality pulmonary angiogram. Besides excellent imaging of lung vascularity, post-contrast VIBE is useful for lung cancer staging and assessment of pleural disease.

Development of the VIBE sequence continues. The latest achievement is CAIPIRINHA (Controlled Aliasing in Parallel Imaging Results in Higher Acceleration) VIBE. CAIPIRINHA VIBE decreases acquisition time leading to decrease in

Table 1: Standard proton MRI chest protocol [2]

Sequence	Plane	Key Pathology and Uses	Spatial Resolution	Temporal Resolution
HASTE	Coronal	Consolidation, masses	Low	High
TrueFISP	Coronal	Pulmonary embolism, respiratory mechanics, gross pulmonary evaluation	Moderate	High
BLADE	Axial	Nodules and masses, bronchial mucous plugging, localized edema	Moderate	Moderate
VIBE	Axial +/- Coronal	Nodules, masses, and consolidation; +/- contrast; pulmonary embolism (+contrast)	High	Low
HASTE	Coronal	Consolidation, masses	Low	High

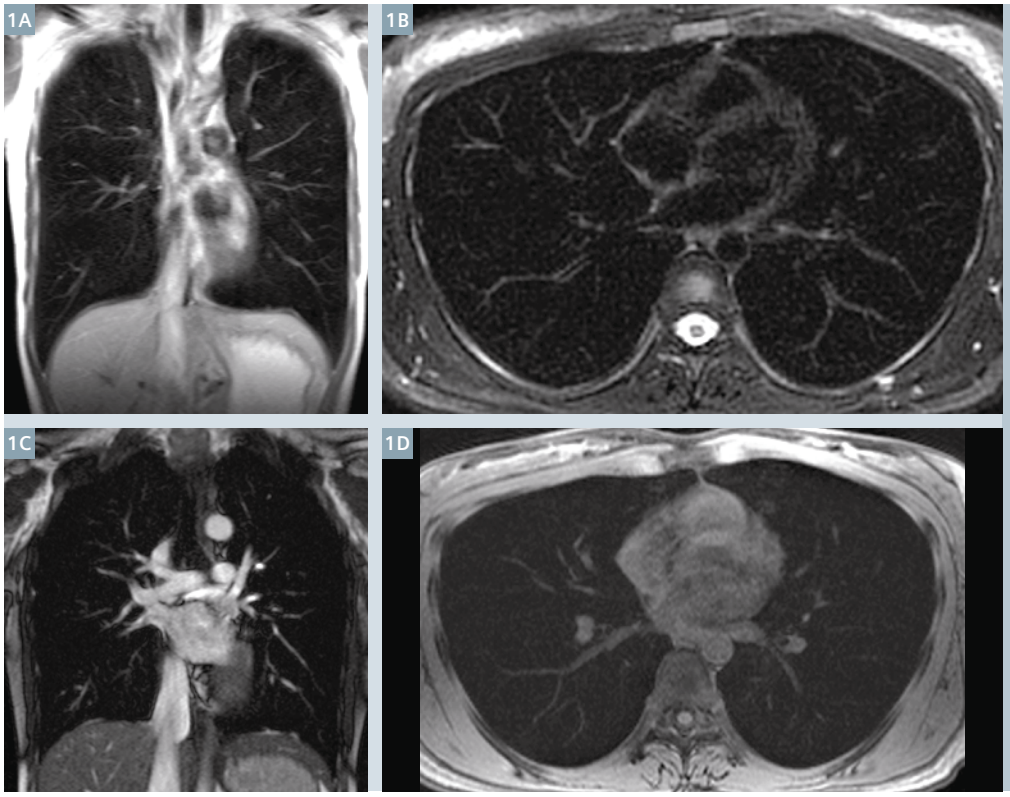

1 Non-contrast pulmonary MRI study in a normal volunteer shows the typical appearance of normal lung parenchyma on HASTE **(1A)**, BLADE **(1B)**, TrueFISP **(1C)**, and VIBE **(1D)** sequences.

breathhold time and increases signal in the mediastinum and central lung compared to standard VIBE. CAIPIRINHA VIBE is especially helpful in highly dyspneic patients in whom a long breathhold is not feasible.

The HASTE sequence is also helpful in detecting pulmonary conditions which increase proton density, and may also nicely show air-trapping due to small airway disease. TrueFISP is a 'white blood' cine sequence with high temporal resolution. In our protocol, the TrueFISP sequence is performed during free-breathing, which allows for assessment of respiratory mechanics; moreover, it is a useful sequence for gross pulmonary assessment in those who cannot hold their breath and as a gross screen for pulmonary arterial filling defects in cases of pulmonary embolism.

BLADE is a T2-weighted turbo spin echo sequence that collects data in radial 'blades' greatly decreasing sensitivity to motion. This sequence is helpful to detect fluid, edema, and/or inflammation (including bronchial inflammation, mucous plugging, and effusions) in addition to other proton-rich conditions of the thorax. As a variation to the protocol, navigator-triggered versions of this sequence are available for imaging of completely uncooperative subjects such a small children.

Proton MRI in chronic lung disease and chronic infection

Cystic fibrosis

Cystic fibrosis (CF) is a common autosomal recessive systemic condition which causes bronchiectasis and predisposes patients to recurrent pneumonia. Life expectancy in CF patients continues to increase with more aggressive therapy and now extends past middle age. Given their increased life expectancy, ionizing radiation should be minimized in CF patients. Proton MRI is a viable alternative to CT in these patients [3-5]. Bronchiectasis, mucous plugging, consolidation, cavities, and localized lung scarring are all evident using standard MRI sequences (Figs. 2, 3). Air-trapping is often evident on HASTE imaging given the relatively large contrast in proton density between normal lung and air-trapped lung in CF patients (Fig. 4).

Sarcoidosis

Sarcoidosis is a systemic illness which causes collections of noncaseating granulomas. The chest is affected in most cases. Pulmonary sarcoidosis manifests as perilymphatic diffuse nodular disease, often with symmetric mediastinal lymphadenopathy. In chronic cases, pulmonary involvement may evolve into frank fibrosis. Proton MRI may be a viable alternative to CT in the imaging of sarcoidosis (Figs. 5-7). Our data showed a strong correlation between MRI and CT, with a Spearman correlation coefficient of 0.774 ($p < 0.0001$) and a Cohen's weighted kappa score of 0.646 [6]. Correlation and agreement were highest for gross parenchymal opacification (consolidation and atelectasis) and lowest for nodular lung disease, though in our experience, significant nodular disease is readily detected using proton MRI, especially if IV contrast is used

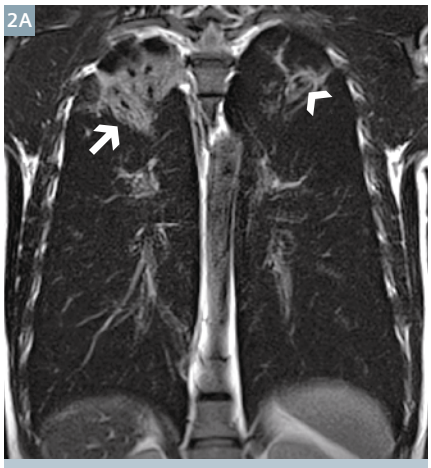

2 Coronal BLADE image in a patient with cystic fibrosis shows intermediate-density consolidation and volume loss in the right upper lobe (arrow). A small cavitary nodule is present in the left upper lobe (arrowhead).

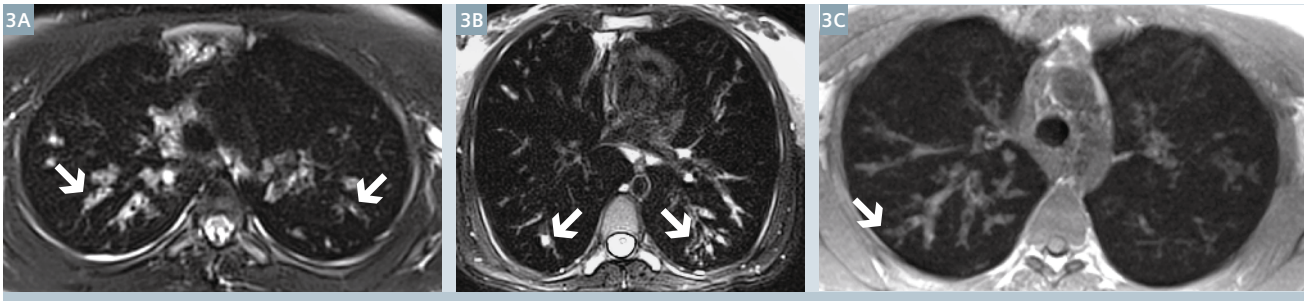

3 Axial BLADE images **(3A, B)** in a patient with cystic fibrosis show bilateral areas of bronchiectasis and mucus plugging (arrows). The T2-weighting of the BLADE sequence allows for accurate identification of inflammatory conditions within the lung parenchyma and airways. Axial VIBE image **(3C)** shows mucous plugging in areas of bronchiectasis out to the subpleural lung in the right upper lobe (arrow). The superior spatial resolution of the VIBE sequence compared to other MRI sequences is helpful in assessing smaller pulmonary structures.

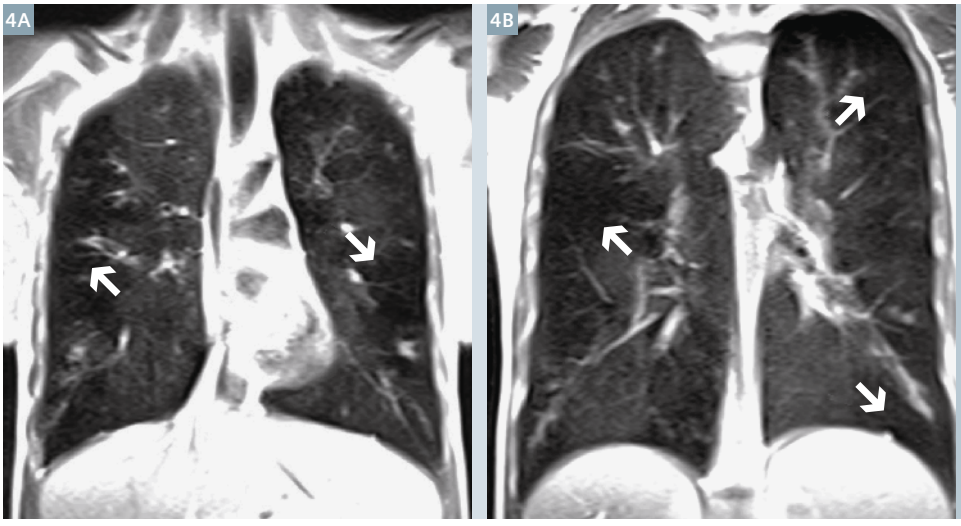

4 Coronal HASTE images **(4A, B)** in a patient with cystic fibrosis shows peripheral areas of relative hypointensity (arrows), consistent with air-trapping.

(Fig. 6). A potentially unique sign of sarcoidosis on proton MRI is the dark lymph node sign which is most evident on post-gadolinium VIBE and T2-BLADE images. This sign was present in approximately half of sarcoidosis cases in our series [7] (Fig. 7).

Nontububerculous mycobacterial pneumonia

Nontububerculous mycobacteria (NTM) are ubiquitously present in the environment including soil, water, and air. In contrast to Mycobacterium tuberculosis, NTM pneumonia is typically not transmissible from person-to-person. NTM presents with bronchiectasis, bronchial thickening, tree-in-bud nodules, cavities, consolidation, and ground-glass opacity on imaging; mirroring those of CF (Figs. 8-10). Patients with NTM pneumonia usually have long life expectancy though progressive disease may lead to significant pulmonary scarring or complete lung destruction. NTM pneumonia patients are imaged semi-annually at our clinical center. Given the high frequency of imaging, proton MRI is an especially attractive alternative to CT in these patients. Our initial data suggests that the correlation between CT and MRI for patients with Mycobacterium Avium Complex pneumonia (the most common type of NTM pneumonia) is strong (0.8252, p-value <0.001) even in the setting of nodular lung disease (Spearman 0.8122, p-value <0.001). Proton MRI's high performance in the setting of nodular disease was surprising as nodules in the setting of NTM pneumonia are quite small, on the scale of 2-4 mm (ATS 2014). We postulate that since nodules in this condition tend to cluster together in a tree-in-bud pattern or in adjacent centrilobular rosettes, the additive signal of adjacent nodules may aid in increasing conspicuity of the nodular disease on proton MRI. The same phenomenon of clustered nodular disease can be seen in many other conditions such as tuberculosis and fungal infection, implying that proton MRI may play a role in these diseases as well.

Miscellaneous

Hypersensitivity pneumonitis

Hypersensitivity pneumonitis is inflammatory disease caused by inhalation of organic or inorganic particles. Common antigenic agents include animal proteins, microbial agents, and low molecular weight chemicals. Imaging findings on chest CT include ground-glass nodules, classically, centrilobular in distribution [8-11]. Concomitant air trapping and mosaic attenuation is quite common occurring in up to 95% of cases. Given the relatively subtle imaging findings of hypersensitivity pneumonitis, one would not expect proton MRI to resolve the pulmonary mani-

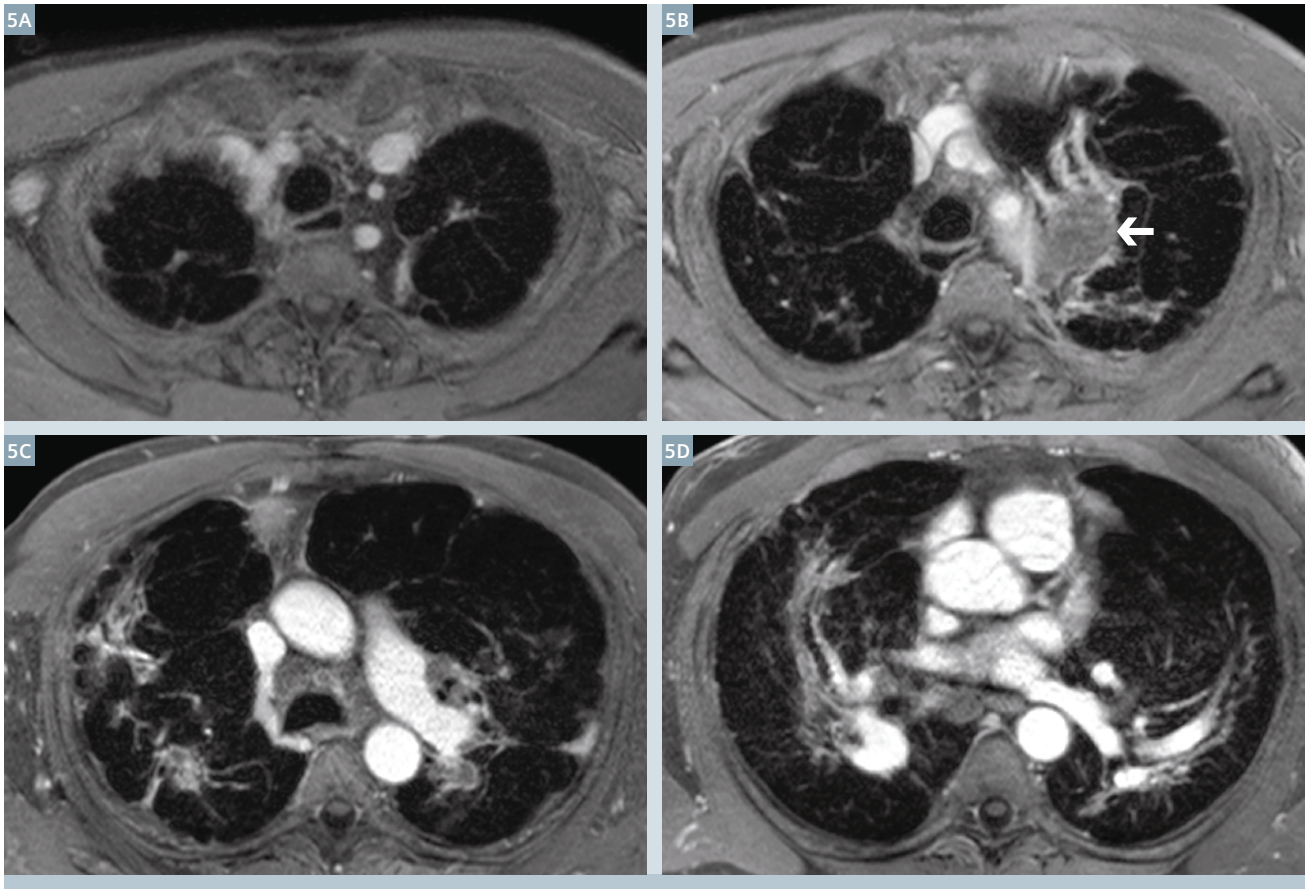

5 Axial post-gadolinium VIBE images **(5A-D)** in a patient with sarcoidosis show mid and upper lung fibrosis and subtle mid lung nodularity with an area of low-intensity, mass-like fibrosis (arrow) in the left upper lobe **(5B)**. Fibrosis is peribronchovascular in axial distribution, typical of chronic sarcoidosis. Low intensity within mediastinal lymphadenopathy likely represents fibrosis or calcification.

festations of this condition. However, with recent advances in MRI technology, even these subtle findings can be detected as shown in Figure 11.

Malignant disease

With the advent of hybrid PET/MRI, there has been renewed interest in whole-body MRI's role in metastatic disease work-up and characterization of specific lesions as benign or malignant. There is strong evidence that proton MRI has potential in differentiating benign from malignant disease in the lungs [12-15]. Given the superior soft tissue contrast of MRI as compared with CT, differentiation between tumor and lung atelectasis is better performed with MRI in cases of central lung masses and invasion of adjacent non-pulmonary structures is readily identified (Fig. 12) [14]. Furthermore, diffusion-weighted imaging (DWI) can help differentiate malignant from benign lung lesions, indicate the type of histology of primary lung cancer, and may increase sensitivity for small pulmonary lesions, for example, in the setting of metastatic disease [14, 16, 17] (Fig. 13). In screening for pulmonary malignancy, CT has superior spatial resolution compared to proton MRI. The lower limit of detectability for pulmonary nodules on proton MRI has been reported to be approximately 5 mm [18-20]. However, with current MRI technology, it may be as low as 4 mm based on our clinical experience; importantly, 6 mm is the threshold of actionable indeterminate pulmonary nodules in lung cancer screening as recommended by Lung-RADS (http://www.acr.org/Quality-Safety/Resources/LungRADS). Given the low signal background of MRI and DWI images, pulmonary nodules which are subtle on CT may be obvious on MRI (Fig. 13).

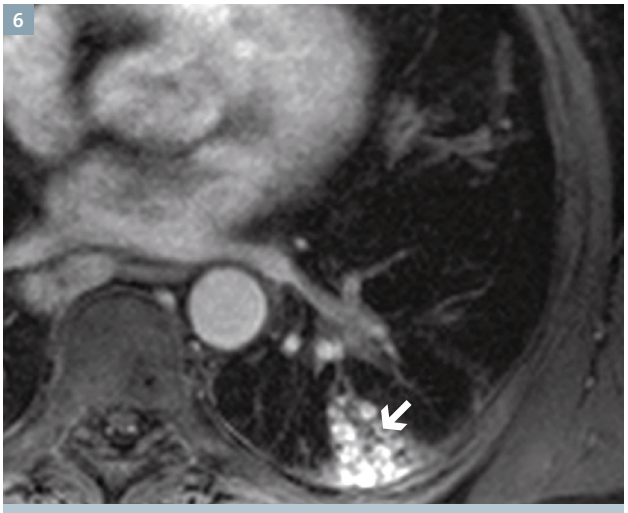

6 Axial post-gadolinium VIBE image clearly shows left lower lobe nodularity (arrow) in this patient with pulmonary sarcoidosis.

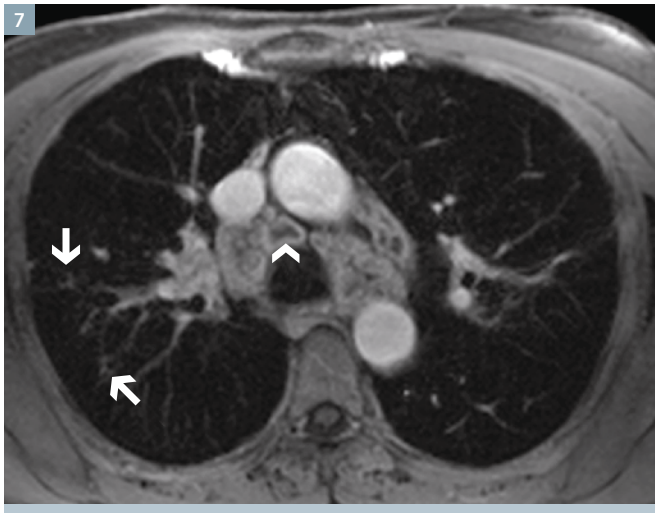

7 Post-gadolinium axial VIBE image shows mediastinal and right peribronchial lymphadenopathy as well as subtle right upper lobe bronchvascular nodularity (arrows) consistent with sarcoidosis. The non-homogeneous nodal enhancement pattern with central hypointensity and peripheral enhancement is known as the dark lymph node sign (arrowhead), which is quite common in lymphadenopathy from sarcoidosis and may potentially be a specific sign for sarcoidosis-related mediastinal lymphadenopathy.

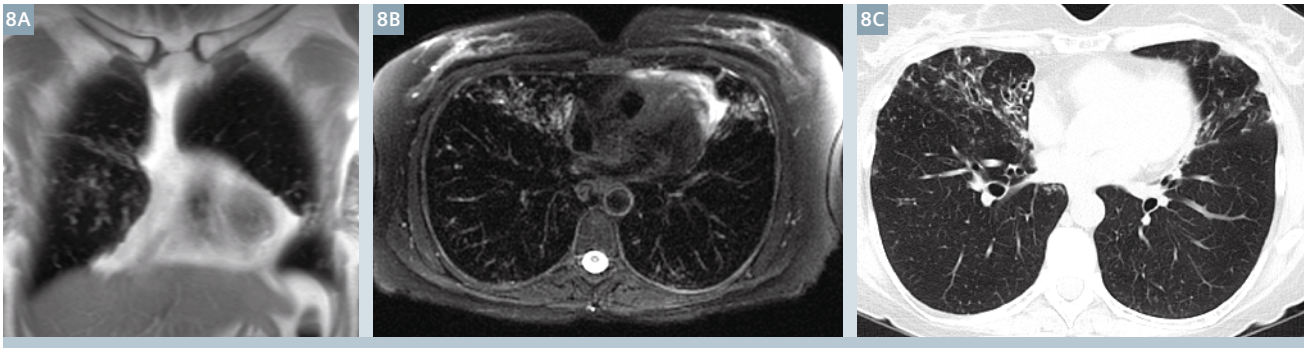

8 Coronal HASTE **(8A)** and axial BLADE **(8B)** MRI images show bronchiectasis in the paracardiac portions of the lungs in this patient with MAC pneumonia. Axial image from chest CT **(8C)** demonstrates bronchiectasis in the same distribution as on MRI.

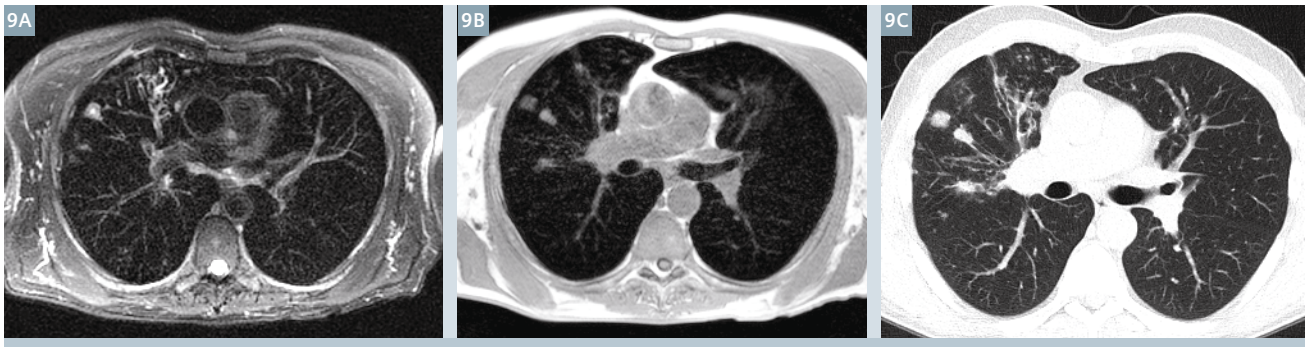

9 Axial BLADE **(9A)** and VIBE **(9B)** MRI images show nodular opacities and bronchiectasis in the right upper lobe in this patient with MAC pneumonia. Axial image from chest CT **(9C)** demonstrates similar imaging manifestations as shown on the MRI images.

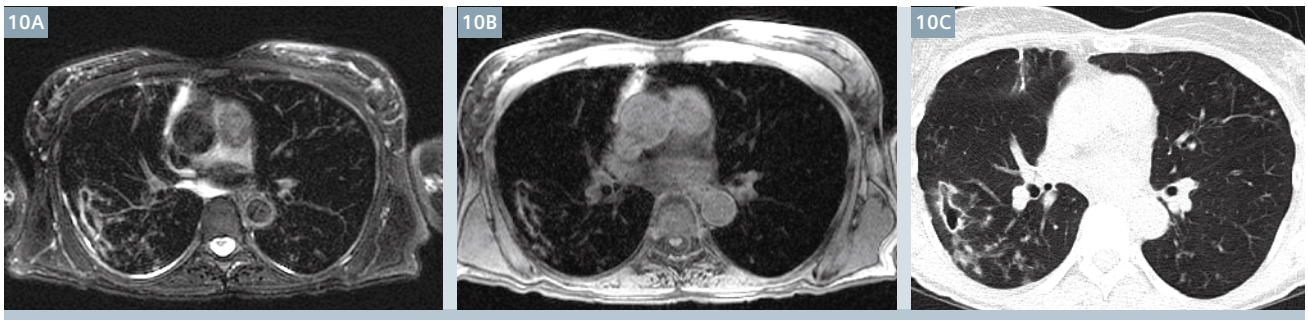

10 Axial BLADE **(10A)** and VIBE **(10B)** MRI images show a focal cavity in the superior segment of the right lower lobe in this patient with MAC pneumonia. Axial image from chest CT **(10C)** again redemonstrates the right lower lobe cavity.

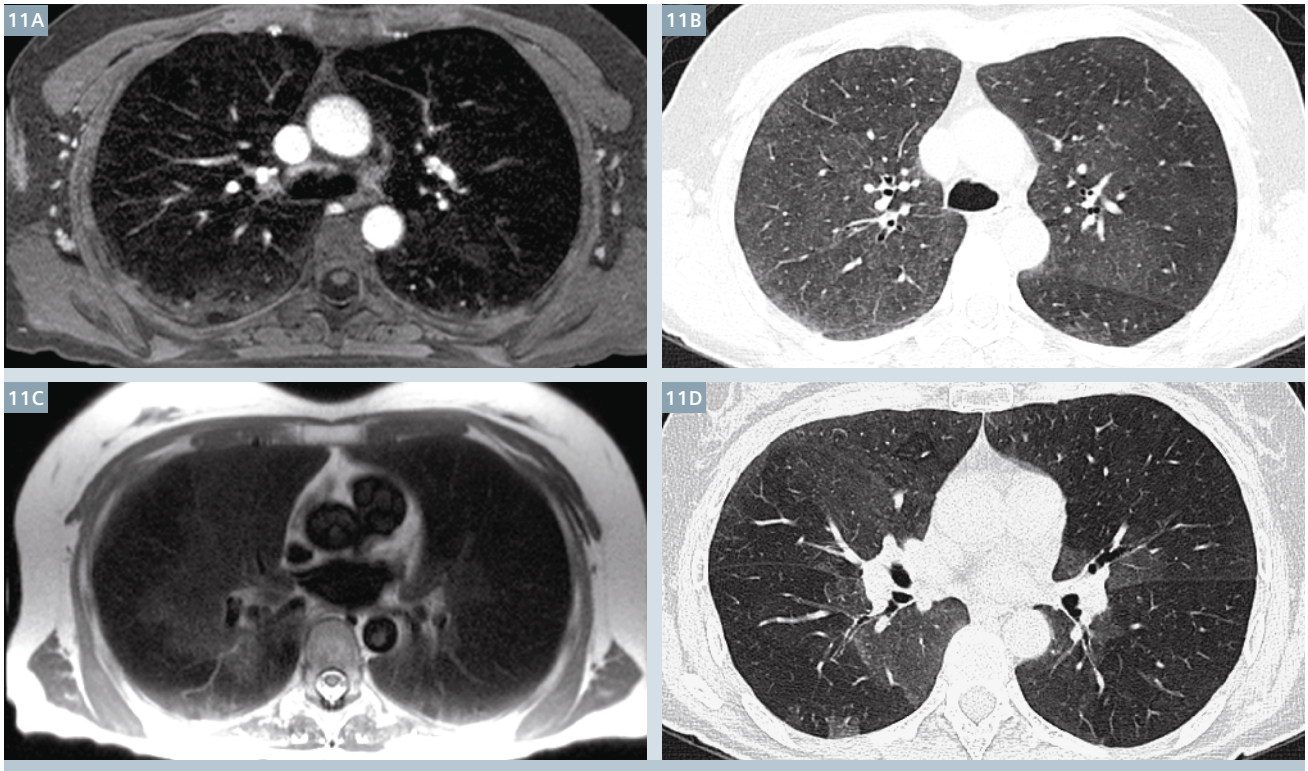

11 Axial post-gadolinium VIBE **(11A)** image shows subtle areas of asymmetric right-sided centrilobular nodularity corroborated on CT **(11B)**. Axial HASTE image **(11C)** from the same patient shows a mosaic pattern with areas of different intensity primarily in the right lung, in a similar distribution as on expiratory CT, consistent with air-trapping **(11D)** in this patient with hypersensitivity pneumonitis.

Pleural disease

Pleural scarring or thickening is most often due to evolution of previous empyema or hemothorax and is usually associated with parenchymal bands or focal rounded atelectasis. Pleural disease is also quite common in the setting of asbestos exposure along with more focal pleural plaques. As a tertiary and quaternary center for chronic lung diseases, our clinical center cares for a large population of patients with collagen vascular disease. Many patients with collagen vascular disease, specifically rheumatoid arthritis, develop pleuritis with resultant pleural scarring. Pleural scarring or thickening may result in restrictive respiratory physiology. Given the long life expectancy of patients with collagen vascular disease related pleural disease, longitudinal follow-up of these patients with CT is suboptimal given the cumulative radiation dose. MRI is a viable tool to follow patients with chronic pleural disease (Fig. 14).

Practical advantages and disadvantages compared to chest CT

The obvious strength of MRI compared to CT is the absence of ionizing radiation. Under the ALARA principle, physicians should do their best to reduce radiation dose to patients while still providing high quality care to patients. Therefore, if MRI can provide similar performance compared to CT in a specific disease setting, physicians should use proton MRI in place of CT. For example, in patients who are at risk for lung cancer, pneumonia should be followed to resolution given that adenocarcinoma may mimic bacterial pneumonia on imaging; MRI could be used to follow these patient rather than CT (Fig. 15). In young patients or in those with contraindication to iodinated contrast, MRA is an excellent means to detect pulmonary arterial thromboembolic disease [21]. As aforementioned, post-contrast VIBE produces excellent images with clear detection of pulmonary emboli (Fig. 16). TrueFISP has inherent white-

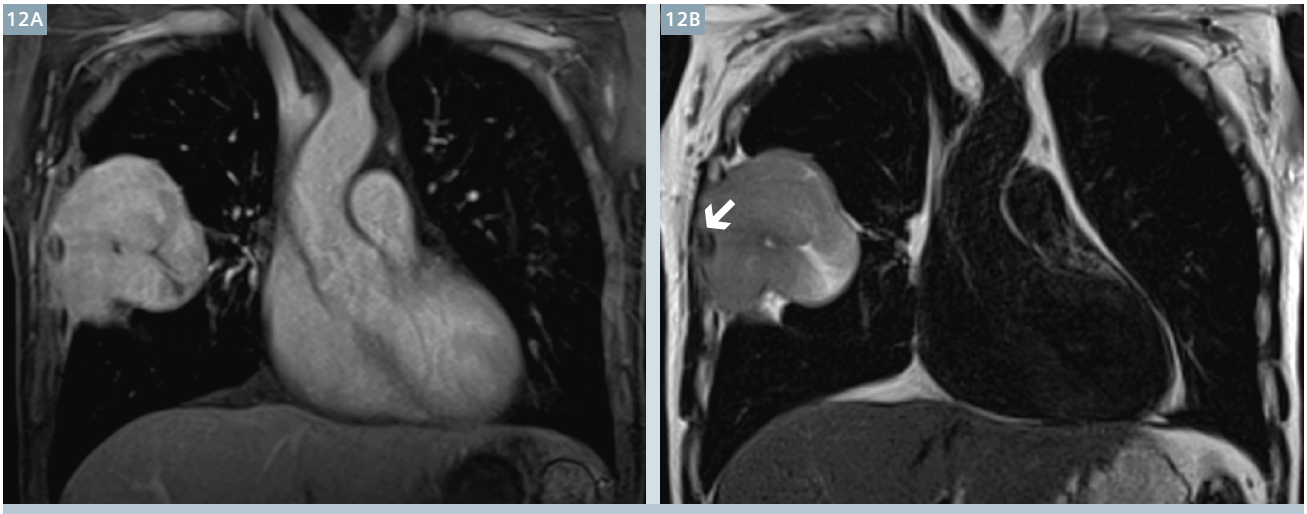

12 Post-gadolinium coronal VIBE **(12A)** and coronal BLADE **(12B)** images show a large mass in the lateral aspect of the right lung invading the adjacent chest wall in this patient with non-Hodkin lymphoma. The encased right lateral rib (arrow) shows abnormal low signal relative to other ribs diagnostic of bone invasion. *(Images courtesy of University Hospital Kiel, Germany.)*

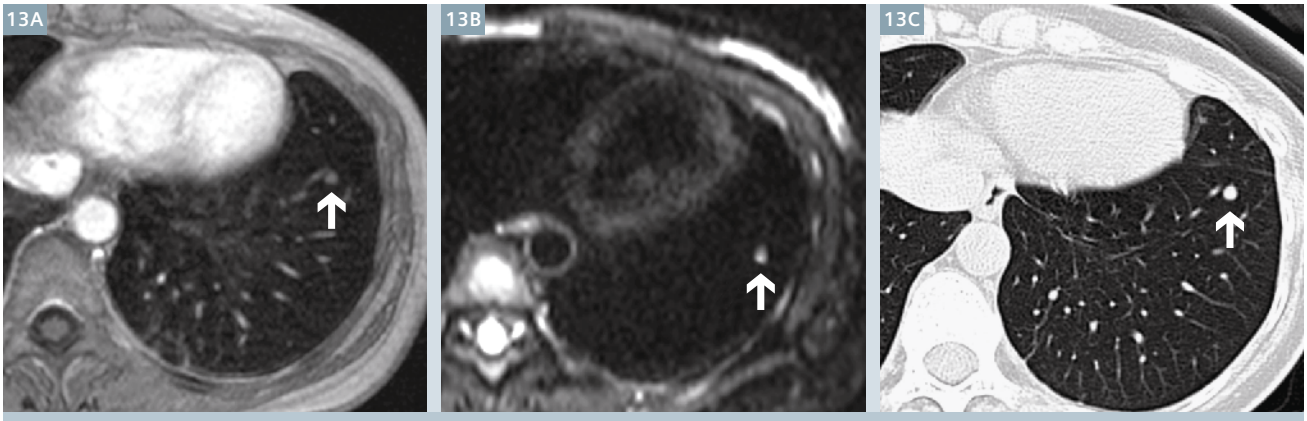

13 Post-gadolinium VIBE axial image **(13A)** shows a 4 mm left lower lobe nodule (arrow) in this patient with metastatic sarcoma. Navigator axial DWI image **(13B)** shows restricted diffusion in this nodule (arrow). The absence of substantial background signal on this sequence increases conspicuity of this lesion; the same lesion (arrow) was not prospectively identified on the axial CT image **(13C)** interpreted at an outside institution.

blood characteristics and can be used to evaluate for central pulmonary embolism in the setting of contrast allergy or renal failure.

However, the benefits of MRI extend beyond radiation reduction. MRI offers superior soft tissue contrast resolution as compared to CT. This stems from the fact that CT imaging is dependent on electron density primarily, whereas MRI imaging derives from proton density and the complex relationship of these protons in different tissues and in magnetic fields. T2-weighted imaging allows MRI to detect areas of localize edema, fluid, or inflammation which are often subtle or invisible on CT. In the setting of anterior mediastinal lesions, microscopic fat within focal tumor-like regions can confirm benign disease using in and out of phase imaging (Fig. 17). Also, MRI offers functional information such as real-time diaphragmatic functional analysis, temporal perfusion, and segmental ventilation, which would be untenable using CT given the resultant high patient radiation exposure.

Currently, MRI cannot match the spatial resolution of CT, though as previously stated, proton MRI can reliably detect nodules on the range of 4-5 mm. Nodules smaller than this are usually not actionable, given the high likelihood of benign disease in nodules smaller than 4 mm. Also, whether MRI can be a useful tool in interstitial lung disease (ILD) has yet to be determined, though isolated use of proton MRI in this setting is likely not currently feasible given the subtle manifestation of early ILD.

One of the biggest hurdles in widespread adoption of thoracic proton MRI is likely financial. Currently, most insurance companies do not explicitly cover proton MRI for general pulmonary assessment. Coverage for lung cancer staging, mediastinal mass, and pleural/chest wall assessment appears to be standard, however. Some would also argue that MRI is more expensive than CT, and therefore, even if MRI performs comparably to CT in pulmonary assessment, CT should be favored. Given that

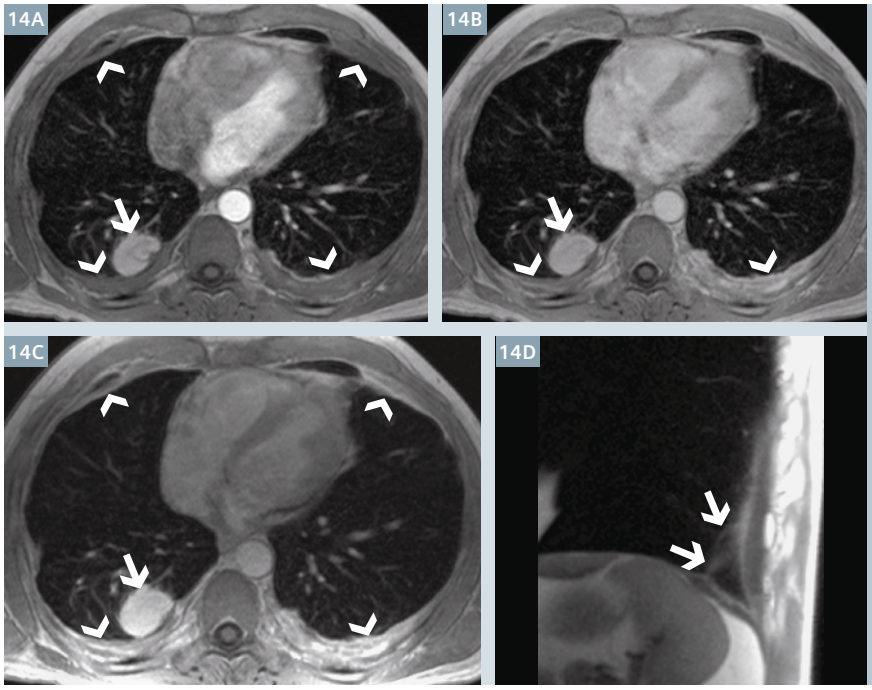

14 Post-gadolinium VIBE axial image at approximately 2, 5, and 7 minutes after contrast administration **(14A-C**, respectively) show progressive enhancement of bilateral pleural thickening (arrowheads) and a focus of rounded atelectasis (arrows) in the right lower lobe in this patient with rheumatoid arthritis. The area of rounded atelectasis can be definitely diagnosed on MRI given the underlying pleural thickening, localized and lobar volume loss, the subpleural location of the mass, and the swirling of the vasculature around this mass; swirling of lung parenchyma within this mass is clearly present on the 2-minute image **(14A)**. Sagittal HASTE image **(14D)** shows low-intensity left-sided pleural thickening with wispy parenchymal bands (arrows) extending centrally from the subpleural lung.

15 Axial T2 BLADE **(15A)**, axial non-contrast VIBE **(15B)**, axial CT **(15C)** images demonstrate left lower lobe consolidation consistent with pneumonia in this patient with fever and chills. Consolidation resolved with antibiotic treatment. For high-risk patients in whom consolidation must be followed to resolution, MRI is an ideal modality given its superior contrast resolution relative to radiography and its radiation-free technique.

most general pulmonary MRI studies can be performed in less than 15-20 minutes, one could make the argument that the cost of MRI should in fact be similar to that of CT in the thorax. In the long run, the strengths and relatively minor weaknesses of thoracic proton MRI suggest that increased coverage, support, and utilization of proton MRI in the thorax is inevitable.

Conclusion

Though CT is the current gold standard modality to image the chest; Proton MRI is a viable means to image the chest including the lungs and pleura. This is especially poignant in patients with long life expectancy who may require chronic follow-up imaging of the chest. As MRI technology progresses, more widespread utilization of proton MRI is expected.

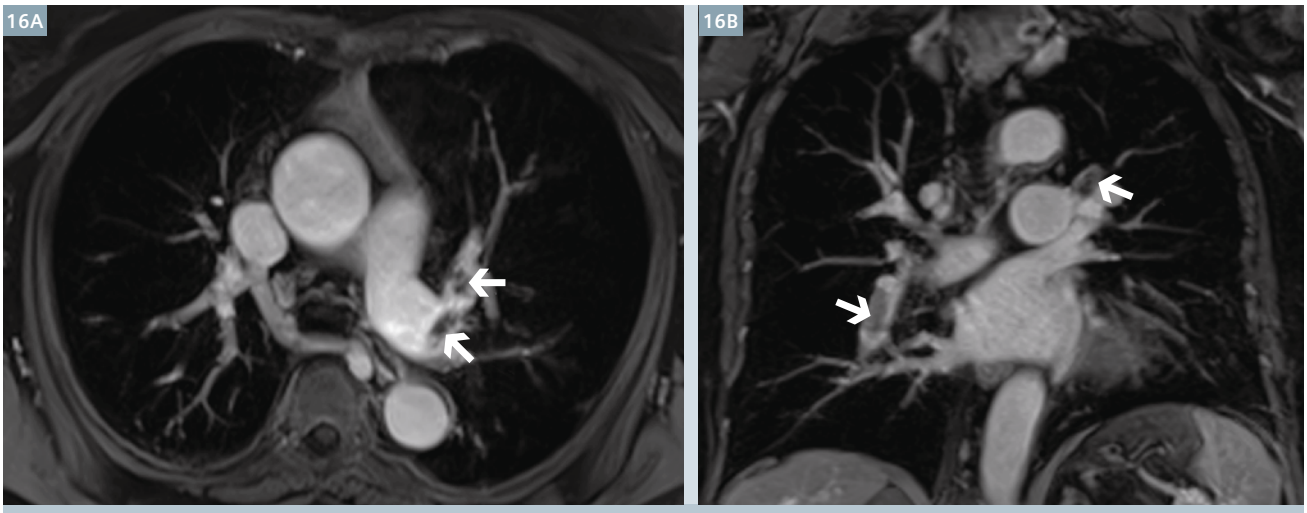

16 Post-gadolinium maximum intensity projection (MIP) VIBE axial **(16A)** and coronal **(16B)** images show filling defects within the pulmonary arteries consistent with pulmonary embolism. CT iodinated contrast was contraindicated as the patient was a candidate for radioiodine therapy for severe hyperthyroidism. In young patents, angiographic imaging using MRI is also valuable in that it allows for detection of pulmonary embolism without use of ionizing radiation.
(Images courtesy of Radiologie Darmstadt, Germany.)

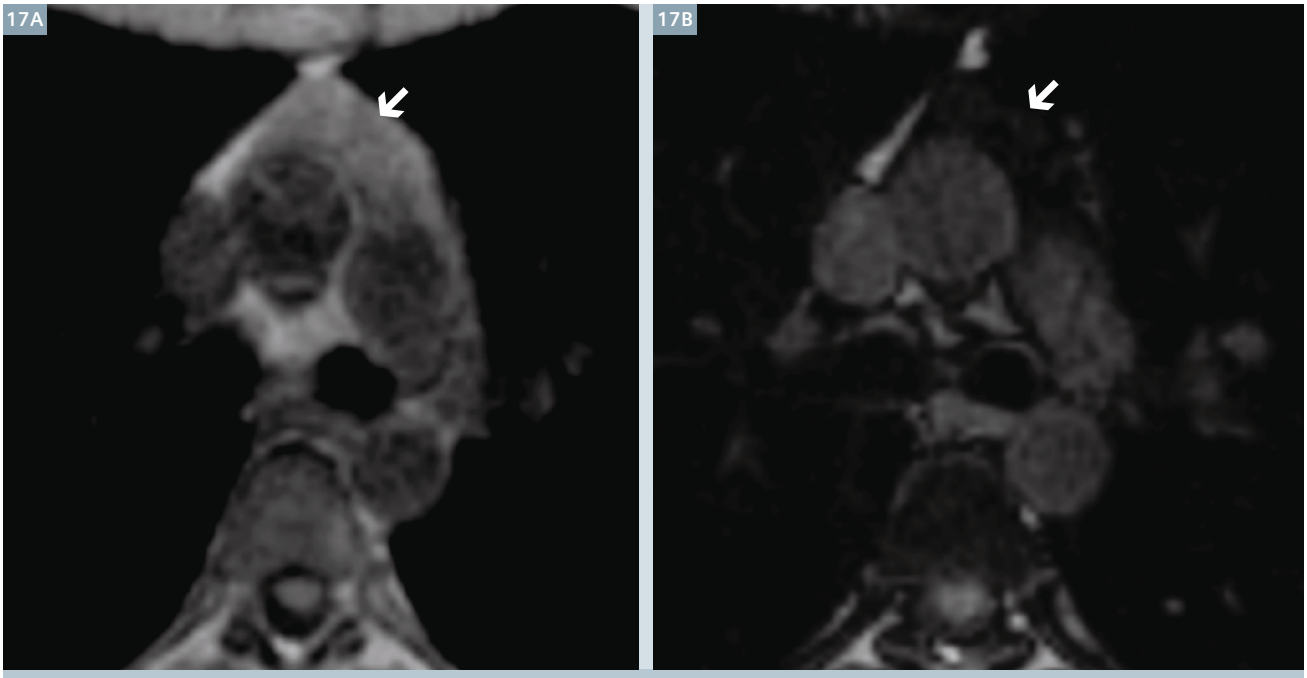

17 In phase **(17A)** and out of phase **(17B)** MR images show a mass lesion (arrows) in the anterior mediastinum. The intensity of the lesion decreases markedly on the out of phase image **(17B)** as compared to the in phase image **(17A)**, implying the presence of a large degree of microscopic fat within the lesion, highly suggestive of thymic hyperplasia as opposed to thymoma.
(Case courtesy of Jeanne B. Ackman, M.D.; Massachusetts General Hospital, Boston, MA, USA.)

References

1. Preston DL, Ron E, Tokuoka S, et al. Solid cancer incidence in atomic bomb survivors: 1958-1998. Radiat Res 2007;168:1-64.
2. Biederer J, Beer M, Hirsch W, et al. MRI of the lung (2/3). Why ... when ... how? Insights Imaging 2012;3:355-371.
3. Eichinger M, Optazaite DE, Kopp-Schneider A, et al. Morphologic and functional scoring of cystic fibrosis lung disease using MRI. Eur J Radiol 2011;81:1321-1329.
4. Failo R, Wielopolski PA, Tiddens HA, Hop WC, Mucelli RP, Lequin MH. Lung morphology assessment using MRI: a robust ultra-short TR/TE 2D steady state free precession sequence used in cystic fibrosis patients. Magn Reson Med 2009;61:299-306.
5. Puderbach M, Eichinger M, Haeselbarth J, et al. Assessment of morphological MRI for pulmonary changes in cystic fibrosis (CF) patients: comparison to thin-section CT and chest x-ray. Invest Radiol 2007;42:715-725.
6. Chung JH, Little BP, Forssen AV, et al. Proton MRI in the evaluation of pulmonary sarcoidosis: comparison to chest CT. Eur J Radiol 2013;82:2378-2385.
7. Chung JH, Cox CW, Forssen AV, Biederer J, Puderbach M, Lynch DA. The dark lymph node sign on magnetic resonance imaging: a novel finding in patients with sarcoidosis. J Thorac Imaging 2013;29:125-129.
8. Lynch DA, Rose CS, Way D, King TE, Jr. Hypersensitivity pneumonitis: sensitivity of high-resolution CT in a population-based study. AJR Am J Roentgenol 1992;159:469-472.
9. Remy-Jardin M, Remy J, Wallaert B, Muller NL. Subacute and chronic bird breeder hypersensitivity pneumonitis: sequential evaluation with CT and correlation with lung function tests and bronchoalveolar lavage. Radiology 1993;189:111-118.
10. Small JH, Flower CD, Traill ZC, Gleeson FV. Air-trapping in extrinsic allergic alveolitis on computed tomography. Clin Radiol 1996;51:684-688.
11. Silva CI, Churg A, Muller NL. Hypersensitivity pneumonitis: spectrum of high-resolution CT and pathologic findings. AJR Am J Roentgenol 2007;188:334-344.
12. Li B, Li Q, Chen C, Guan Y, Liu S. A systematic review and meta-analysis of the accuracy of diffusion-weighted MRI in the detection of malignant pulmonary nodules and masses. Acad Radiol 2013;21:21-29.
13. Coolen J, Vansteenkiste J, De Keyzer F, et al. Characterisation of solitary pulmonary lesions combining visual perfusion and quantitative diffusion MR imaging. Eur Radiol 2013;24:531-541.
14. Yang RM, Li L, Wei XH, et al. Differentiation of central lung cancer from atelectasis: comparison of diffusion-weighted MRI with PET/CT. PLoS One 2013;8:e60279.
15. Chen L, Zhang J, Bao J, et al. Meta-analysis of diffusion-weighted MRI in the differential diagnosis of lung lesions. J Magn Reson Imaging 2012;37:1351-1358.
16. Sommer G, Tremper J, Koenigkam-Santos M, et al. Lung nodule detection in a high-risk population: comparison of magnetic resonance imaging and low-dose computed tomography. Eur J Radiol 2013;83:600-605.
17. Tanaka R, Nakazato Y, Horikoshi H, et al. Diffusion-weighted imaging and positron emission tomography in various cytological subtypes of primary lung adenocarcinoma. Clin Imaging 2013;37:876-883.
18. Biederer J, Both M, Graessner J, et al. Lung morphology: fast MR imaging assessment with a volumetric interpolated breath-hold technique: initial experience with patients. Radiology 2003;226:242-249.
19. Heye T, Ley S, Heussel CP, et al. Detection and size of pulmonary lesions: how accurate is MRI? A prospective comparison of CT and MRI. Acta Radiol 2012;53:153-160.
20. Schroeder T, Ruehm SG, Debatin JF, Ladd ME, Barkhausen J, Goehde SC. Detection of pulmonary nodules using a 2D HASTE MR sequence: comparison with MDCT. AJR Am J Roentgenol 2005;185:979-984.
21. Biederer J, Mirsadraee S, Beer M, et al. MRI of the lung (3/3)-current applications and future perspectives. Insights Imaging 2012;3:373-386.

Contact

Jonathan Hero Chung, M.D.
Associate Professor, Department of Radiology
Director of Pulmonary MRI
Director of Radiology Professional Quality Assurance
Director of Cardiopulmonary Imaging Fellowship
National Jewish Health
1400 Jackson Street
Denver, CO 80206
USA
Chungj@njhealth.org

Further information

For protocols, clinical talks by renowned experts, articles and case studies, please visit us at

www.siemens.com/magnetom-world-lung